Effects of Milling Condition on the Surface Integrity of Hot Forged Steel

Alessandro R. Rodrigues
roger@dem.feis.unesp.br
São Paulo State University – UNESP
Engineering Faculty of Ilha Solteira
15.385-000 Ilha Solteira, SP, Brazil

Hidekasu Matsumoto
hidekasu@dem.feis.unesp.br

Wyser J. Yamakami
wyser@dem.feis.unesp.br

Rafael Gustavo da R. Paulo
rgrpaulo@yahoo.com.br

Cleiton Lazaro F. de Assis
clfassis@aluno.feis.unesp.br

This paper presents a study on the influence of milling condition on workpiece surface integrity focusing on hardness and roughness. The experimental work was carried out on a CNC machining center considering roughing and finishing operations. A 25 mm diameter endmill with two cemented carbide inserts coated with TiN layer were used for end milling operation. Low carbon alloyed steel Cr-Mo forged at 1200 °C was used as workpiece on the tests. Two kinds of workpiece conditions were considered, i.e. air cooled after hot forging and normalized at 950 °C for 2 h. The results showed that finishing operation was able to significantly decrease the roughness by at least 46% without changing the hardness. On the other hand, roughing operation caused an increase in hardness statistically significant by about 6%. The machined surface presented deformed regions within feed marks, which directly affected the roughness. Surface finish behavior seems to correlate to the chip ratio given the decrease of 25% for roughing condition, which damaged the chip formation. The material removal rate for finishing operation 41% greater than roughing condition demonstrated to be favorable to the heat dissipation and minimized the effect on material hardness.
***Keywords**: high-speed cutting, milling, hardness, roughness, surface integrity*

Introduction

Researches on high-speed cutting (HSC) were initially performed by Carl J. Salomon who machined non-ferrous materials by using a big-diameter circular tool (Flom and Komanduri, 1989; Schützer and Schulz, 2004). Salomon evaluated some of the advantages when applying HSC such as decrease of temperatures and cutting forces, which can be decisive on workpiece surface integrity. Meantime, the results of Salomon related to cutting temperature have been discussed scientifically since his findings (Longbottom and Lanhan, 2006).

HSC is a relative term which depends on the workpiece material and on the chip formation process. According to Flom and Komanduri (1989), HSC for a given material can be defined scientifically as that speed above which shear localization develops completely in the primary shear zone. For soft workpieces HSC generates continuous chips, while difficult-to-cut materials develop segmented ones. From an industrial standpoint, HSC is defined in terms of cutting speed ranges, where cutting speed is elevated and feed per tooth and depth of cut are diminished aiming at finishing and semi-finishing operations (Schulz, 1999; Müller and Soto, 1999; Tönshoff et al. 2001). The transition between conventional cutting speed and HSC is still not entirely clear.

Despite the progress regarded for HSC, many scientific results are still contradictory, in such areas like machining phenomena and workpiece surface integrity. Blümke, Sahm and Müller (2001) milling the spheroidized and pearlitic steel 40CrMnMo7 (180 and 260 HV respectively) up to 4000 m·min^{-1} concluded that increasing the cutting speed resulted in an increase of chip segmentation and hardness. Sahm and Siems (2001) milling the same material affirm that chip segmentation caused diminution on cutting force levels with a cutting speed increase, which can affect less the surface machined given the lower mechanical effect. Biesinger et al. (2001) state that the strengthening of the subsurface layer was not found by hardness measurements when milling the steel 40CrMnMo7 and the increase in cutting speed caused a reduction in roughness. Chakraborty et al. (2008) verified an increase of about 16% on surface hardness, when end milling steel AISI 4340 in dry conditions. Finally, according to Flom and Komanduri (1989) there are indications that surface finish tends to improve with increasing cutting speed, but these results are not conclusive.

The objective of this research was to understand the behavior of roughness and hardness as a function of cutting condition and workpiece material. Chip ratio, material removal rate and heat distribution were also evaluated aiming to contribute to the analysis.

Nomenclature

A	= *air cooled workpiece*
a_e	= *width of cut, mm (in)*
a_p	= *depth of cut, mm (in)*
f_z	= *feed per tooth, mm/tooth (in/tooth)*
N	= *normalized workpiece*
Q	= *material removal rate, cm^3·min^{-1} (in^3·min^{-1})*
R_a	= *centerline average roughness, μm (μin)*
r	= *chip ratio, dimensionless*
r_ε	= *tool corner radius, mm (in)*
t	= *undeformed chip thickness, mm (in)*
t_c	= *medium chip thickness, mm (in)*
v_c	= *cutting speed, m·min^{-1} (in·min^{-1})*

Greek Symbols

α	= *ferrite or Widmanstatten ferrite*
α_o	= *tool orthogonal clearance angle, deg*
β	= *pearlite*
χ_r	= *tool cutting edge angle, deg*

Experimental Work

The tests were carried out on a Romi CNC machining center model Discovery 560. The main features are 11 kW power, 10000 rpm maximum spindle rotation and 30 m·min^{-1} maximum feed speed. A 25 mm diameter endmill with two cemented carbide inserts coated with TiN layer (code R390-11 T3 08M-PM 4030 and

Paper accepted August, 2009. Technical Editor: Anselmo Eduardo Diniz

grade ISO P25) from Sandvik Company was employed for the endmill operation adopting a down-milling condition. The tool dimensional characteristics are 21° orthogonal clearance angle (α_o), 0.8 mm corner radius (r_ε) and 90° cutting edge angle (χ_r).

Two cutting conditions were applied on the tests in order to clearly differentiate the roughing (lower cutting speed and higher depth of cut and feed per tooth) and finishing (high-speed cutting and lower depth of cut and feed per tooth). All machining tests were performed in dry condition with 5 mm width of cut (a_e) and linear tool path in the x-axis direction only. Table 1 summarizes the cutting parameters which were based on ranges indicated in Sandvik Coromant (1999), Tönshoff et al. (2001) and Chevrier et al. (2003).

Table 1. Cutting parameters used on machining tests.

Parameter	Unit	Milling Conditions	
		Roughing	Finishing
Depth of cut (a_p)	mm	1.5	1.0
Feed per tooth (f_z)	mm/tooth	0.15	0.08
Cutting speed (v_c)	$m \cdot min^{-1}$	100	400
Material removal rate (Q)	$cm^3 \cdot min^{-1}$	1.58	2.24

A new cutting edge was used for each test to assure the equal initial conditions since tool wear has not been considered as a testing variable and it should not interfere on the tool behavior during milling operations. All milling tests were executed twice and hardness and roughness values were measured six times for each milling condition and replica to allow the statistical analysis.

The workpiece surface finish was determined considering the parameter R_a. The roughness meter from Mitutoyo Company model SJ-201P was used on the measurements adopting 0.8 mm cut-off and 5 μm needle radius. In addition, a workpiece surface visual characterization was also performed aiming to compare the visual surface texture to the quantitative roughness measurements. The milled surface images were obtained by a Carl Zeiss Jena optical microscope model Neophot 21.

The hardness was measured by a tester from Heckert Company with load of 98 N in the Vickers scale and loading time of 15 s. The indentations were obtained at room temperature on the basis of ASTM E 92-92 standard.

The chip ratio (r) given by Eq. (1) was measured three times in each one of three chips representatives from all cutting conditions by using the aforementioned optical microscope. The chosen chips were cross-sectionally cupped in polyester resin, sanded with granulometry 400 and 600, polished with aluminum oxide of 1 μm particle size and etched with reagent Nital 2% during 5 s.

$$r = \frac{t}{t_c} \tag{1}$$

where t [mm] is the undeformed chip thickness and t_c [mm] is the medium chip thickness.

The cutting temperature at the cutting zone was estimated on the basis of specific cutting energy. The cutting force was measured by a Kistler piezoelectric 3-component dynamometer model 9257BA and signal conditioner model 5233A. The F_x, F_y and F_z components were recorded at 1 kHz sample rate by a National Instruments acquisition board A/D model PCI-MIO-16E-4 and software Labview®. To calculate the specific cutting energy, the force signals were integrated numerically by the trapeze method along the cutting time and multiplied by the ratio between cutting speed and removed workpiece volume.

In accordance with Shaw (2004), considering that 97 to 99% of mechanical energy is converted into thermal energy, the cutting temperature T_c could be estimated by solving Eq. (2) which is derived from the First Law of Thermodynamic:

$$u = \rho \int_{T_i}^{T_c} C(T)\,dT \tag{2}$$

where u [J/m^3] is specific cutting energy, ρ [kg/m^3] is workpiece specific mass, T_i [°C] is initial temperature before milling, T_c [°C] is cutting temperature at the cutting zone during milling and C [kJ/kg·K] is specific heat. To extract the cutting temperature T_c, the specific heat was fitted by an exponential curve ($R^2 = 0.972$) along to cutting temperature variation. Specific mass value and specific heat range were obtained for the milled workpiece material from Incropera and DeWitt (2006). Finally, to estimate the heat dissipation, the workpiece surface temperatures were immediately measured before and after tests by using a contact thermocouple type K (Chromel-Alumel) and an acquisition system calibrated to operate between 0 and 1000 °C.

Workpiece Material

Low carbon alloyed steel Cr-Mo provided by an automotive industry was initially shared in a billet shape, pre-heated in an induction furnace, hot forged at 1200 °C and submitted to tumbling operation for cleaning. This route is commonly carried out by the industry in order to prepare the blanks metallurgically and geometrically for subsequent machining stage. Two sample conditions were considered in this work, i.e. air cooled immediately after hot forging and normalized at 950 °C for 2 h designed as (A) and (N), respectively. The normalizing treatment is used in industry and air cooling was adopted as a possibility for eliminating the thermal treatment.

It is relevant emphasizing that cylindrical workpieces employed in milling tests are remaining portions of gears, clutches and brakes with real dimensions produced by industry. Thus, the end milling operation used in this work aimed to simulate the machining of contours, slots and pockets carried out on the face of these components. Table 2 shows the material chemical composition and Fig. 1 illustrates the geometry of blank and pre-machined workpieces.

Table 2. Workpiece chemical specification (wt %).

C	Mn	Cr	Mo	Si	P	S
0.23 0.28	0.90 1.30	0.35 0.70	0.10 0.20	0.15 0.35	0.25 max	0.02 0.04

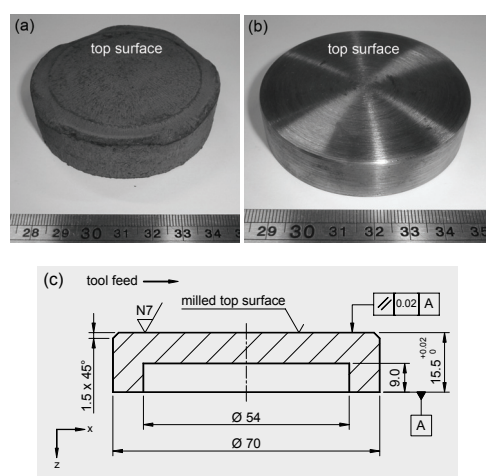

Figure 1. Workpiece shapes: (a) blank, (b) pre-machined and (c) final dimensions for tests.

For microstructural characterization, the workpieces were cross-sectionally sawed by an abrasive disc, cupped in polyester resin and sanded by sandpapers with granulometry 120, 220, 400, 600 and 1000. After, the specimens were polished with aluminum oxide of 1 μm particle size and etched using reagent Nital 2% by 20 and 5 s for workpieces (A) and (N), respectively. The microstructure images were also obtained by the optical microscope above mentioned. Figure 2 shows the microstructures of the specimens.

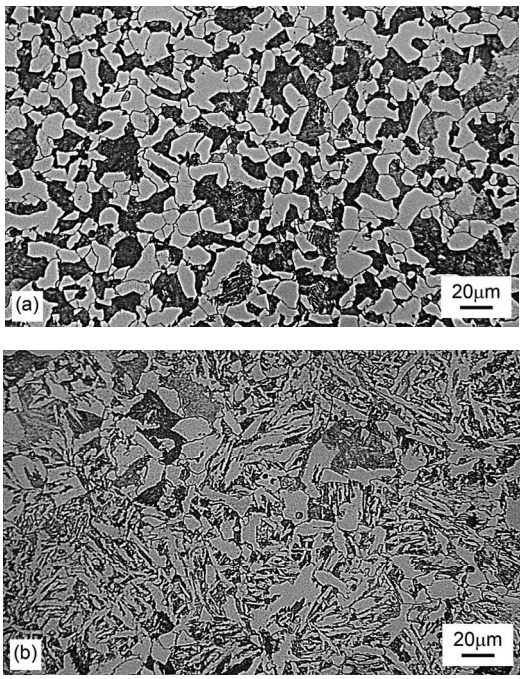

Figure 2. Microstructure of samples (a) normalized and (b) air cooled (Nital 2% etching).

The microstructure of condition (N) presents a matrix composed predominantly of ferrite and pearlite in clear and dark colors, respectively, with well-defined grain contours (Fig. 2a). The morphology of ferrite and pearlite is polygonal or equiaxial with few occurrences of slightly stretched and irregular grains. Figure 2b shows the microstructure of condition (A) that has a more prolonged morphology characterizing a predominant acicular structure. Because of higher cooling rate, when compared to condition (N), the microstructure is formed of a clear-color Widmanstatten ferrite and a dark-color pearlite. These microconstituints display an adverse shape varying from stretched on the majority of the area to polygonal on isolated regions.

Table 3 concludes microstructural characterization of the workpieces providing the volume fraction and mean grain size. All quantitative results were determined by applying the ASTM E 112-95 and E 562-95 standards. The condition (A) presents a more refined microstructure with ASTM (G) grain size around 12 against 10 of workpiece (N). Due to ferrite predominance in both microstructures (approximately 60%), it is possible to discern that hardness is not elevated, as it will be seen ahead. However, when comparing two conditions, it can be noticed that workpiece condition (A) presents greater hardness values than condition (N) due to presence of the Widmanstatten ferrite in the microstructure. The hardness results will be discussed forward.

Table 3. Quantitative metallography of workpieces.

Workpiece condition	Volume fraction (%)		Mean grain size [μm]*	
	α^{**}	β	α^{**}	β
(A)	63	37	5.5 (12)	7.2 (11.5)
(N)	57	43	8.6 (11)	11.2 (10)

* ASTM (G) grain size in parentheses.
** Widmanstatten ferrite in (A) and Polygonal ferrite in (N).

Results and Discussion

Workpiece Surface Finish

The roughness results obtained in this work presented equal tendencies to those divulged in scientific literature, when finishing operation using high-speed cutting is researched (Tönshoff et al., 2001; Schulz, Abele and Sahm, 2001; Schützer and Schulz, 2004; Rodrigues and Coelho, 2007 and Amin et al., 2007). Figure 3 shows a synthesis about the roughness behavior in the tests. It is possible to examine the graph according to either workpiece or cutting conditions. The medium experimental error was 8.8% for a 95% confidence level.

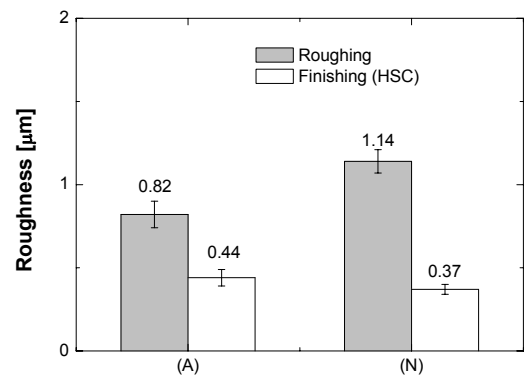

Figure 3. Influence of workpiece and milling condition on roughness.

The 300% increase in cutting speed associated especially to the feed per tooth reduction by 47% (finishing operation) decreased the workpiece roughness by around 46.3% and 67.5% on average for workpieces (A) and (N) respectively. The roughness decrease is most likely associated to the sum of effects such as greater frequency of insert passages over milled workpiece surface given the lower feed per tooth, smoother tool geometry and better chip formation due to elevated cutting speed.

Considering the effect of cutting condition on the microstructure, an opposite tendency for machined materials is verified. Roughness increased by 39.0% at roughing, but decreased by 15.9% at finishing when analyzed from conditions (A) to (N). A more detailed examination of machined surface is given in Fig. 4a and 5a indicating that workpiece (N) (with greater roughness) displayed a great number of irregular feed marks.

The origin of these damages caused by low cutting speed in roughing operation can be associated to the difficulty of chip formation, i.e., the chip was formed not only by complete shear process, but also likely by an undesirable plastic flow such as plowing effect or side flow. This fact may have generated a non-uniform surface where the tool action on machined regions deformed the material surface. It is relevant emphasizing that carbide inserts were substituted in each test to assure identical machining conditions. Furthermore, tool wear and built-up edge occurrences were not detected as well as irregularities on the tool and workpiece fixation system.

Figures 4b and 5b representative of workpiece (N) machined under finishing condition presented a uniform surface with equally spaced feed marks. Note that the machined surface does not contain marks such as in the previous case, hence a decisive fact for obtaining better roughness.

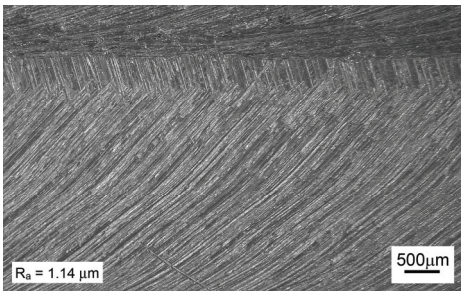

(a) Roughing for sample (N)

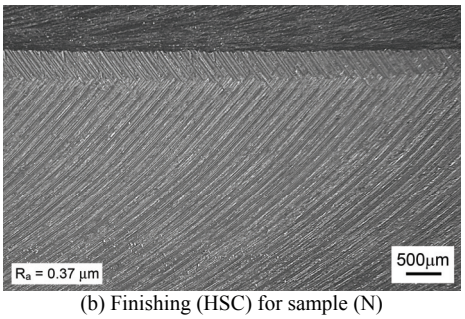

(b) Finishing (HSC) for sample (N)

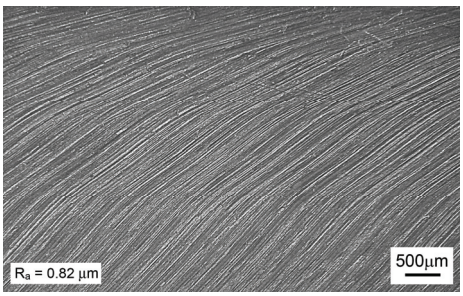

(c) Roughing for sample (A)

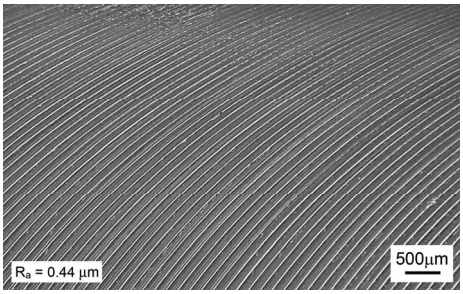

(d) Finishing (HSC) for sample (A)

Figure 4. Surface texture of tested workpieces (2x magnification).

Figures 4c and 5c present sample surface (A) considering roughing operation. Analogous to Figs. 4a and 5a, it is possible to observe some irregularities regarding feed marks very likely generated by non-uniformity during chip formation. Once the irregularity level was smaller, the roughness could be improved probably because of the larger workpiece hardness and refined microstructure. Finally, Figs. 4d and 5d display the workpiece surface (A) machined under HSC condition (finishing operation). Again, the easiness of the material cutting on account of high speed and low tool feed caused a regular pattern of feed marks and decreased the specimen roughness.

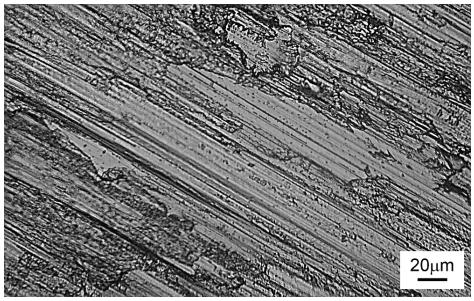

(a) Roughing for sample (N)

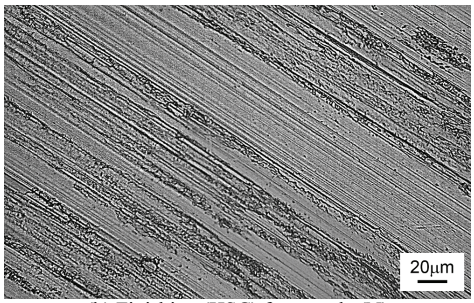

(b) Finishing (HSC) for sample (N)

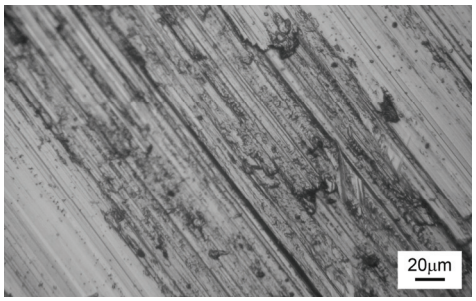

(c) Roughing for sample (A)

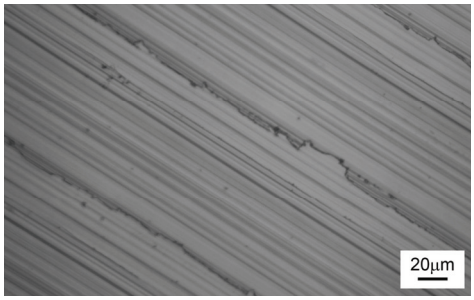

(d) Finishing (HSC) for sample (A)

Figure 5. Surface texture of tested workpieces (500x magnification).

The final analysis of milled surface roughness is shown in Fig. 6. The machined surface seems to indicate slight undulations that are more pronounced in samples milled under roughing operation. Additionally, the microstructural characterization conducted in the cross-section of the machined surface reveals that both cutting conditions did not cause alterations in the pearlite/ferrite morphology nor phase transformations near the milled surface when compared to the matrix texture presented in Fig. 2.

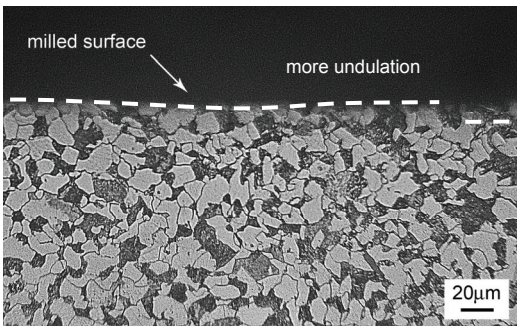

(a) Roughing for sample (N)

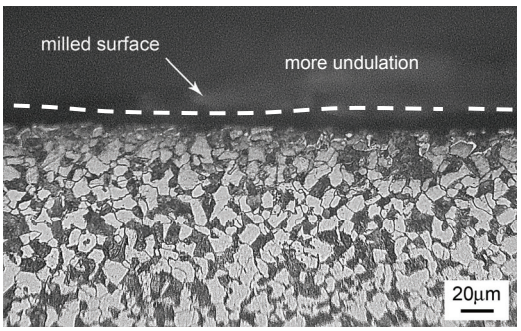

(b) Finishing (HSC) for sample (N)

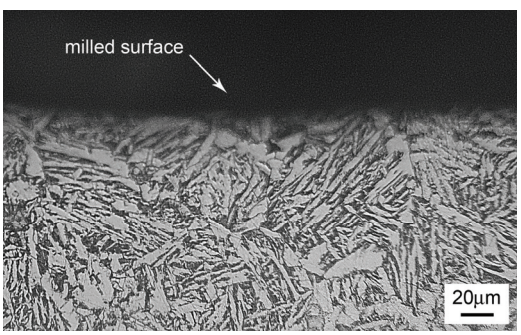

(c) Roughing for sample (A)

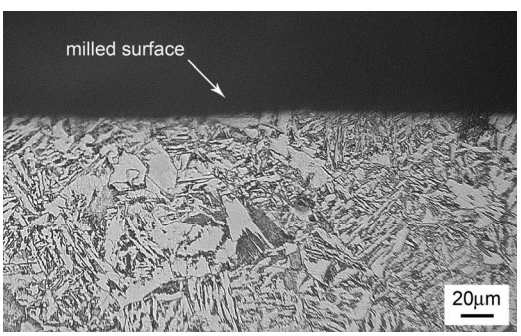

(d) Finishing (HSC) for sample (A)

Figure 6. Microstructure of workpieces near milled surface (Nital 2% etching).

Workpiece Material Hardness

The influence of the cutting condition on workpiece hardness is summarized in Fig. 7. The graph can be comprehended according to two aspects, i.e., by comparing tested microstructure and cutting conditions. All hardness results present an experimental error of about 1.7% for a 95% confidence level.

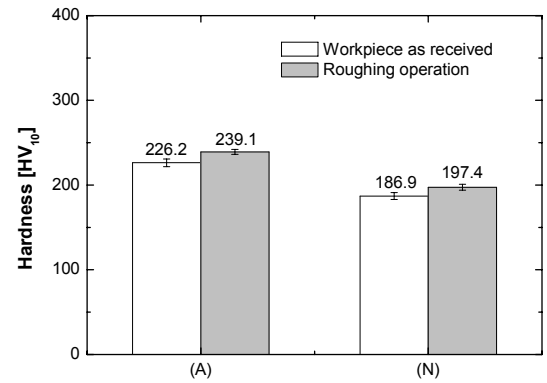

(b) Finishing operation (HSC)

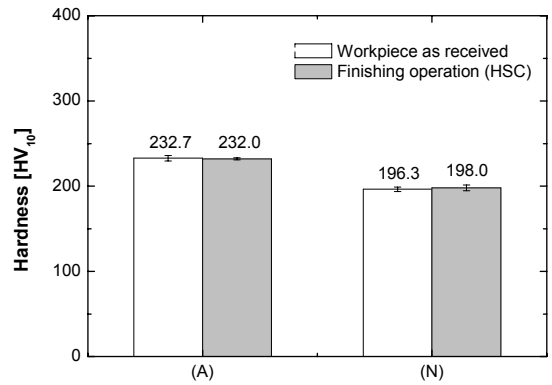

(a) Roughing operation

Figure 7. Effect of the milling condition on machined workpiece hardness.

Firstly, when considering the microstructure analysis in Fig. 7a and 7b, it can be observed that workpiece condition (A) presented greater hardness values than those for workpieces (N) increasing by around 18.7% on average. This occurred due to a microstructural distinction generated by different cooling rates. In other words, the specimens (A) presented Widmanstatten ferrite grains containing microconstituints of smaller mean grain size and acicular morphology.

The cutting condition applied on the tests presented an influence considered relevant to this research. When comparing hardness results with milling conditions, it is noticed in Fig. 7a that roughing operation caused an increase in hardness of around 5.7% and 5.6% for workpiece conditions (A) and (N), respectively. Although with small percentages, these hardness elevations represent a statically significant result given that they exceed the experimental deviation previously mentioned. When evaluating the hardness behavior in finishing operation (HSC), Fig. 7b illustrates that the greater hardness variation reached only 0.9% approximately, hence statically identical measurements. At first, this result demonstrates that finishing operation using HSC does not influence on surface integrity (hardness) of the machined workpiece.

Finally, the chip ratio and cutting temperature shown in Fig. 8 were also obtained in order to correlate roughness and hardness to the thermomechanical phenomena occurred at the cutting zone.

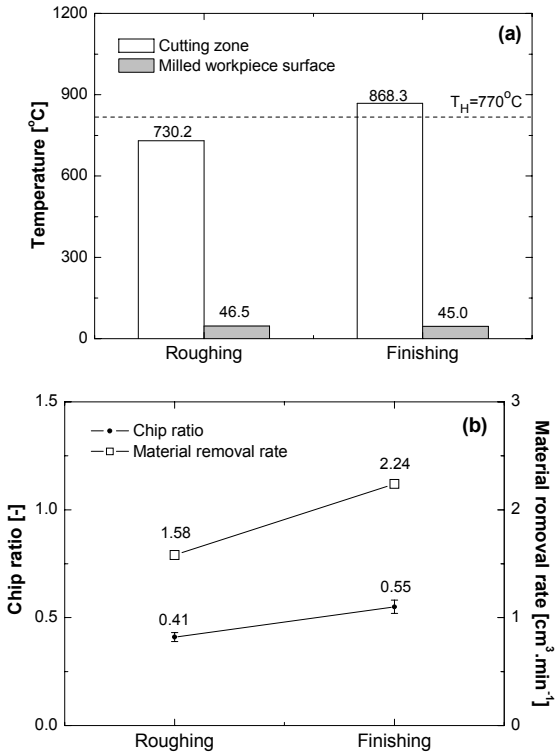

Figure 8. Influence of milling condition on (a) workpiece temperature and (b) chip ratio.

The roughing operation presented a chip ratio 25% lesser than for finishing (Fig. 8b). It demonstrates the chips from roughing condition were more badly-formed than those from finishing using HSC, affecting the roughness and causing mechanical hardening independently of the workpiece material. The material removal rate of 42% greater for finishing than for roughing demonstrates that it is possible to increase productivity without influencing on workpiece hardness.

Figure 8a shows that the material removal rate due to finishing operation using HSC caused temperature elevation around 19% at the cutting zone, exceeding the workpiece homologous temperature (770 °C). According to Shaw (2004), this indicates that finishing took place under hot work condition and was governed by the strain rate, while roughing was performed under cold work and influenced by the strain level.

In addition, it may be observed in Fig. 8a that workpiece surface temperatures for both materials and cutting conditions were approximately equal after milling tests, indicating the heat on account of finishing condition was dissipated by greater removed chip volume and the milled workpiece surface was thermally less affected given also the smaller workpiece-tool contact time. Therefore, the workpiece milling at the cutting zone was simultaneously facilitated given the higher heat and chip ratio.

The dimensional and morphological characteristics of chips for all materials and cutting conditions may be seen in Fig. 9.

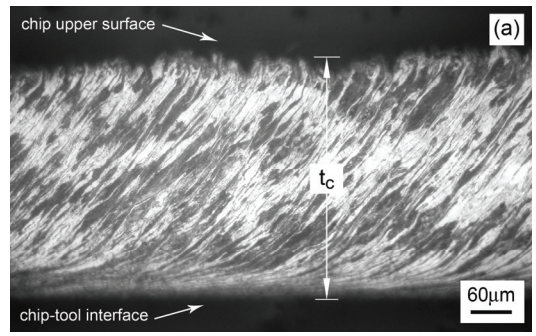

(a) Roughing for sample (N)

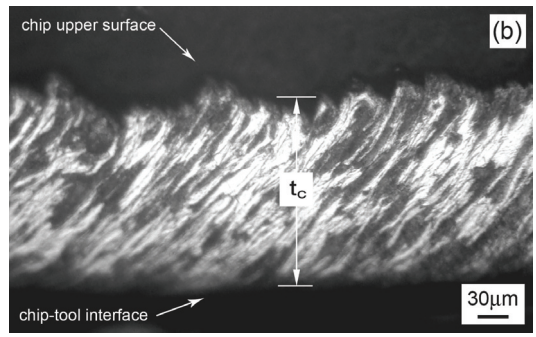

(b) Finishing (HSC) for sample (N)

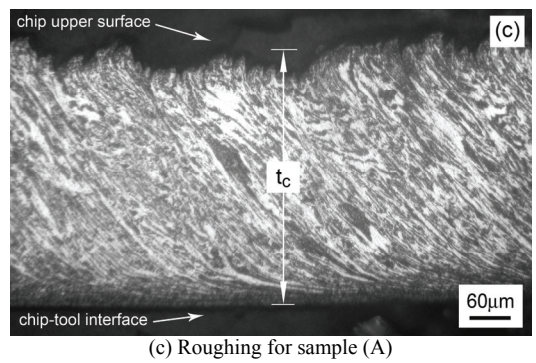

(c) Roughing for sample (A)

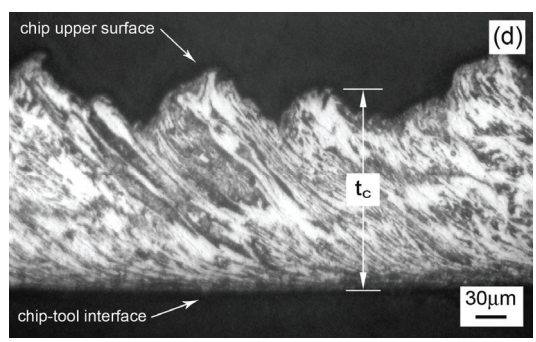

(d) Finishing (HSC) for sample (A)

Figure 9. Effect of milling conditions and workpiece material on chip ratio and morphology.

The cross-section metallography of the roughing chips for both workpiece materials (Fig. 9a and 9c) allows classifying them as continuous with equally distributed ferritic-pearlitic microstructure. There is no clear distinction between lamellae and shear bands, which emphases their continuity. On the other hand, Figs. 9b and 9d indicate evidences of an initial segmentation in the upper surface of chips obtained under finishing operation, mainly for air cooled workpiece (A) given its higher hardness. It may be seen clearly the

thickness of roughing chips is greater than that of finishing ones given the lower cutting speed and higher feed per tooth, hence conducting to a lesser chip ratio for each undeformed chip thickness respective.

Conclusions

Finishing operation using HSC significantly favored the surface roughness for all workpiece conditions improving the roughness by 57% on average. This result was mainly attained due to low feed per tooth, high cutting speed, greater frequency of tool edge passages over machined surface and better chip formation.

The tool activity during the chip formation process demonstrates to be important regarding the machining impact on workpiece surface integrity. Situations of low chip ratio and undesirable plastic flow, such as plowing effect or side flow can cause significant damages to the surface finish and hardness of the workpiece.

Finishing using HSC permitted to increase the material removal rate without modifying the material hardness. However, roughing operation caused an increase on the sample hardness of up to approximately 6%. This can change the mechanical properties of the workpiece and alter its operational behavior.

Cutting temperature can be estimated by measuring the specific cutting energy and applying the First Law of Thermodynamic at the cutting zone. Finishing condition generated 19% more temperature than roughing milling due to increase of the cutting speed and material removal rate. However, the heat was dissipated by removed chip volume and affected less the workpiece surface integrity.

The machining of ductile materials under soft cutting conditions can also affect the workpiece surface integrity.

References

Amin, A.K.M.N, Abraham, I., Khairusshima, N. and Ahmed, M.I., 2007, "Influence of preheating on performance of circular carbide inserts in end milling of carbon steel", *Journal of Materials Processing Technology*, Vol. 185, pp. 97-105.

Biesinger, F., Thiel, M., Schulze, V., Vöhringer, O., Krempe, M. and Wendt, U., 2001, "Characterization of surface and subsurface regions of HSC-milled steel", In: Schulz, H. (Editor), "Scientific Fundamentals of HSC", Ed. Druckhaus, Munich, Germany, pp. 137-149.

Blümke, R., Sahm, A. and Müller, C., 2001, "Influence of heat treatment on chip formation in high speed milling", In: Schulz, H. (Editor), "Scientific Fundamentals of HSC", Ed. Druckhaus, Munich, Germany, pp. 43-52.

Chakraborty, P., Asfour, S., Cho, S., Onar, A. and Lynn, M., 2008, "Modeling tool wear progression by using fixed effects modeling technique when end milling AISI 4340 steel", *Journal of Materials Processing Technology*, Vol.205, pp. 190-202.

Chevrier, P., Tidu, A., Bolle, B., Cezard, P. and Tinnes, J.P., 2003, "Investigation of surface integrity in high speed end milling of a low alloyed steel", *International Journal of Machine Tools and Manufacture*, Vol. 43, pp. 1135-1142.

Flom, D.G. and Komanduri, R., 1989, "High speed machining", In: Davis, J.R. (Editor), "ASM Metals Handbook: Machining", Ohio, USA, Vol. 16, pp. 597-606.

Incropera, F.P. and DeWitt, D.P., 2006, "Fundamentals of Heat and Mass Transfer", Ed. Wiley, USA, 997 p.

Longbottom, J.M. and Lanhan, J.D., 2006, "A review of research related to Salomon's hypothesis on cutting speeds and temperatures", *International of Machine Tools and Manufacturing*, Vol. 46, pp. 1740-1747.

Müller, P. and Soto, M., 1999, "Usinagem sem refrigeração de furos e roscas", Proceedings of the 4th International Seminary of High Tecnology", Santa Bárbara d'Oeste, Brazil, pp. 127-133.

Rodrigues, A.R. and Coelho, R.T., 2007, "Influence of the tool edge geometry on specific cutting energy at high-speed cutting", *Journal of the Brazilian Society of Mechanical Sciences and Engineering*, Vol. 29, No. 3, pp. 279-283.

Sahm, A. and Siems, S., 2001, "Influence of chip segmentation on cutting force", In: Schulz, H. (Editor), "Scientific Fundamentals of HSC", Ed. Druckhaus, Munich, Germany, pp. 151-160.

Sandvik Coromant, 1999, "Fabricação de Moldes e Matrizes", S. Paulo, Brazil, 208 p.

Schulz, H., 1999, "The history of high-speed machining", Proceedings of the 5th International Scientific Conference on Production Engineering, Opatija, Croatia, pp. 2-12.

Schulz, H., Abele, E. and Sahm, A., 2001, "High-speed machining – fundamentals and industrial application", Proceedings of the 6th International Seminary of High Tecnology – Advanced Manufacture, Piracicaba, Brazil, pp. 25-44.

Schützer, K. and Schulz, H., 2004, "The history of high-speed machining", In: Santos, A.V. (Editor), "High-Speed Machining", Ed. Érica, S. Paulo, Brazil, pp. 17-30.

Shaw, M.C., 2004, "Metal Cutting Principles", Oxford University Press, New York, USA, 672 p.

Tönshoff, H.K., Friemuth, T., Andrae, P. and Amor, R.B., 2001, "High-speed or high-performance cutting – a comparison of new machining technologies", *Production Engineering*, Vol. 8, No. 1, pp. 5-8.